Near-perfect nonmagnetic invisibility cloaking

Nina A. Zharova*
Institute of Applied Physics, Russian Academy of Sciences, Nizhny Novgorod, 603950, Russia

Alexander A. Zharov, Jr. and Alexander A. Zharov
Institute for Physics of Microstructures, Russian Academy of Sciences, Nizhny Novgorod, 603950, Russia
(Received 20 June 2013; revised manuscript received 24 September 2013; published 14 November 2013)

We suggest a way to obtain a near-perfect nonmagnetic invisibility cloak structure. Within the particular example of cylindrical geometry and transverse magnetic polarization of light, we show that such a cloak can operate for a cylindrical object of very large diameter, keeping the total scattering cross section limited by $2\lambda/\pi$. We also demonstrate that proposed cloak does not require extremely high values of dielectric permittivity, in contrast to the cloaks designed according to a transformation optics technique.

DOI: 10.1103/PhysRevA.88.053818 PACS number(s): 42.79.−e, 02.40.−k, 42.15.Eq, 42.25.Fx

I. INTRODUCTION

The studies of invisibility cloaking have attracted a great deal of effort in recent years after pioneering works [1,2] that suggested a way of spatial transformation to design material objects invisible to incoming electromagnetic radiation. The basis for this phenomenon is the equivalence between light propagation in curved space and in some particular inhomogeneous and anisotropic optical material. This concept led to a new field of contemporary electromagnetics called transformation optics (TO). The first experiment in microwaves using TO ideas demonstrated that the visibility of the objects can be significantly reduced using properly designed covering metamaterial [3]. In recent years, several different concepts of cloaking of small subwavelength particles have also been suggested [4–8]. One of them is based on the resonant cancellation of the dipole scattering by means of covering the spherical particle with a layer of another material [4–6]. The other concept exploits the coating of the nanoparticle of arbitrary shape and material with a spherical shell of zero-permittivity material to shield it from the incident radiation and suppress its dipole scattering with an extra dielectric layer [7,8]. The latter type of cloak design is highly promising because it does not use magnetic metamaterials and can be realized with only natural homogeneous materials. However, such kind of cloak can operate solely for rather subwavelength-sized particles and it is ineffective for bigger objects due to the higher multipole input to the optical cross section. At the same time, the realization of an invisibility cloak designed by transformation optics is quite challenging. It requires an effective covering medium with identical tensors of dielectric permittivity $\hat{\varepsilon}$ and magnetic permeability $\hat{\mu}$. These tensors have to be anisotropic and spatially inhomogeneous and in two-dimensional case some components of $\hat{\varepsilon}$, $\hat{\mu}$ have to reach infinite values at the inner boundary of the cloak. Actually, the most serious obstacle in constructing such a device is to provide necessary magnetic response. This difficulty can be overcome in the microwave band by exploiting split-ring resonator arrays [9]. Magnetic resonance in the array of ferroelectric cylinders of micron size was suggested for terahertz frequencies [10]. However, for visible and near-infrared light, a strong degeneration of magnetic properties, $\hat{\mu} \to \hat{1}$, takes place even for most of the known artificial metamaterials.

Therefore, efforts in this field focus on design of completely nonmagnetic cloak where the hiding effect is to be reached in a medium with $\hat{\mu} = \hat{1}$. In recent years, numerous works have been published on different types of simplified nonmagnetic cloaking design (see, for example, Refs. [11–13]), which either lead just to the reduction of the scattering cross section or operate only under very specific conditions. Some alternative approximate approaches to the optical cloaking are based upon geometrical optics when only the refractive index is taken into account but not dielectric permittivity and permeability themselves [2,14,15]. Noticeable progress was reached in design of cloaking shells in two-dimensional case by means of quasiconformal transformations for creating the so-called carpet or ground cloak [16]. The efficiency of this kind of cloak was then confirmed not only by numerical simulations but also in real experiments [17–19]. One more design of simplified cloak suitable for two-dimensional (2D) geometry and transverse magnetic (TM) polarization of electromagnetic radiation [14,20,21] incorporates, in a certain sense, TO ideas and a geometrical optics approach, when two components of dielectric tensor and a single component of magnetic tensor are calculated according to TO formulas and then redefined in such a way to keep longitudinal and transverse refraction indices and obtain a purely nonmagnetic medium.

Thus, to date a number of simplified approaches exist, and some of them have been experimentally demonstrated, but they do not provide an appropriate cloaking. Actually only one way is known for *perfect invisibility cloaking* which is based on TO ideology. However, it cannot be realized in optics owing to, in particular, the required identical permittivity and permeability and their extreme values. In this article, we show that modification of the "classical" TO approach allows design of an *ideal nonmagnetic* cloaking shell that ensures invisibility of a cylindrical object irradiated by TM-polarized electromagnetic waves. A *nearly perfect* hiding shell with finite values of dielectric tensor components provides a total scattering cross section, σ, less than $2\lambda/\pi$, independent of the object size. This behavior leads to a possibility of realization of a *nearly perfect macroscopic* invisibility cloak. In contrast to the ground cloak with "limited cloaking potential," [16] the

*zhani@appl.sci-nnov.ru

proposed device is of the "push-forward mapping" [1] kind; it crushes the cloaked object to a point and is relevant to cloaking a localized object.

II. NONMAGNETIC CLOAKING FORMALISM VS TO: 2D CASE

The 2D evolution of a TM-polarized monochromatic electromagnetic wave in a vacuum can be described by the scalar Helmholtz equation for the z component of the magnetic field, H,

$$\frac{1}{r}\frac{\partial}{\partial r}\left(r\frac{\partial H}{\partial r}\right)+\frac{1}{r^2}\frac{\partial^2 H}{\partial \phi^2}+k_0^2 H=0, \quad (1)$$

where r and ϕ are cylindrical coordinates. Following the TO ideas, we want to find some specific transformation $R=R(r)$, $\tilde{H}=\tilde{H}(r,H)$ (keeping ϕ unchanged) which transforms (1) to more general form for magnetic field $\tilde{H}$ in anisotropic nonmagnetic medium with permittivity tensor components $\hat{\varepsilon}_{rr}=\varepsilon_\parallel$, $\hat{\varepsilon}_{\phi\phi}=\varepsilon_\perp$

$$\frac{1}{R}\frac{\partial}{\partial R}\left(\frac{R}{\varepsilon_\perp}\frac{\partial \tilde{H}}{\partial R}\right)+\frac{1}{R^2}\frac{\partial}{\partial \phi}\left(\frac{1}{\varepsilon_\parallel}\frac{\partial \tilde{H}}{\partial \phi}\right)+k_0^2\tilde{H}=0. \quad (2)$$

It reduces the problem of electromagnetic field propagation in a medium with inhomogeneous permittivity tensor $\hat{\varepsilon}$ to the problem of a plane wave propagation in free space, in case such a transformation should be found.

It is convenient to use logarithmic cylindrical coordinates, $\rho=\ln(k_0 r)$, $\tilde{\rho}=\ln(k_0 R)$, since the both Eqs. (1) and (2) take simpler forms:

$$\frac{\partial^2 H}{\partial \rho^2}+\frac{\partial^2 H}{\partial \phi^2}+\exp(2\rho)H=0 \quad (3)$$

and

$$\frac{\partial}{\partial \tilde{\rho}}\left(\frac{1}{\varepsilon_\perp}\frac{\partial \tilde{H}}{\partial \tilde{\rho}}\right)+\frac{\partial}{\partial \phi}\left(\frac{1}{\varepsilon_\parallel}\frac{\partial \tilde{H}}{\partial \phi}\right)+\exp(2\tilde{\rho})\tilde{H}=0. \quad (4)$$

One should note that introducing of auxiliary logarithmic coordinates does not give an additional freedom in transformations. Since $\rho(r)$ and $r(\rho)$ both are single-valued functions, we can use any representation of these two because they are equivalent. Thus, further we make all the calculations using ρ dependencies and finally return to initial radial coordinates.

Assuming that

$$H=G(\rho)\tilde{H}, \qquad \frac{d\rho}{d\tilde{\rho}}=\frac{R dr}{r dR}\equiv g(\rho), \quad (5)$$

with some unknown functions $G(\rho)$, $g(\rho)$ we can rewrite first term of Eq. (3) as

$$\frac{\partial}{\partial \rho}\left(G\frac{\partial \tilde{H}}{\partial \rho}+\tilde{H}\frac{dG}{d\rho}\right)=\tilde{H}\frac{d^2G}{d\rho^2}+\frac{1}{G}\frac{\partial}{\partial \rho}\left(G^2\frac{\partial \tilde{H}}{\partial \rho}\right)$$
$$=\tilde{H}\frac{d^2G}{d\rho^2}+\frac{1}{gG}\frac{\partial}{\partial \tilde{\rho}}\left(\frac{G^2}{g}\frac{\partial \tilde{H}}{\partial \tilde{\rho}}\right). \quad (6)$$

By substituting this expression into Eq. (3) and collecting the terms, we obtain after simple transformation

$$\frac{\partial}{\partial \tilde{\rho}}\left(\frac{G^2}{g}\frac{\partial \tilde{H}}{\partial \tilde{\rho}}\right)+gG^2\frac{\partial^2 \tilde{H}}{\partial \phi^2}+gG\left(\frac{d^2G}{d\rho^2}+Ge^{2\rho}\right)\tilde{H}=0, \quad (7)$$

which coincides with the form of Eq. (4) if the following conditions are satisfied:

$$\varepsilon_\perp=\frac{g}{G^2}, \qquad \varepsilon_\parallel=\frac{1}{gG^2}, \quad (8)$$

and

$$gG\left(\frac{d^2G}{d\rho^2}+G\exp(2\rho)\right)=\exp(2\tilde{\rho}). \quad (9)$$

The expressions (8) define components of the permittivity tensor through the functions $g(\rho)$ and $G(\rho)$. However, taking into account the definition of $g(\rho)$, Eq. (5), notice that the last condition (9) gives the relation between the scaling factor $G(\rho)$ and new logarithmic radial coordinates $\tilde{\rho}(\rho)$. Thus, only one of functions $g(\rho)$, $G(\rho)$ remains unspecified.

Using Eq. (5), one can rewrite Eq. (9) in the form

$$G\left(\frac{d^2G}{d\rho^2}+Ge^{2\rho}\right)=\exp(2\tilde{\rho})\frac{d\tilde{\rho}}{d\rho}\equiv\frac{1}{2}\frac{d}{d\rho}[\exp(2\tilde{\rho})]$$
$$\equiv\frac{1}{2}d\left(k_0^2R^2\right)/d\rho, \quad (10)$$

or in radial coordinates $[R=\frac{1}{k_0}\exp(\tilde{\rho}),\ r=\frac{1}{k_0}\exp(\rho),\ d/d\rho=rd/dr]$,

$$\ddot{G}+\frac{1}{r}\dot{G}+k_0^2G=\frac{k_0^2}{Gr}R\dot{R}, \quad (11)$$

where the dot denotes the derivative over the old coordinate r. Therefore, by defining an *arbitrary* monotonously increasing function $R(r)$ [demanding only matching $R(r)$ with vacuum conditions at the outer boundary of the cloak $R_{\rm ext}$: $R(r=R_{\rm ext})=R_{\rm ext}$, $dR/dr(r=R_{\rm ext})=1$], the problem reduces to the differential equation (11) with boundary conditions $G(R_{\rm ext})=1$, $dG/dr(R_{\rm ext})=0$. The solution of this equation, $G(r)$, and Eqs. (8) allow one to find the components of the tensor $\varepsilon_\perp$, $\varepsilon_\parallel$. Mapping the plane wave in vacuum to the (R, ϕ)-space gives the structure of the magnetic field $\tilde{H}$

$$\tilde{H}(R)=H/G=\frac{1}{G}\exp[ik_x r(R)\cos(\phi)+ik_y r(R)\sin(\phi)] \quad (12)$$

corresponding to diffraction of a unit-amplitude plane wave on cloaked object. Simple calculations determine also the relations between transformed and vacuum electric fields:

$$\tilde{E}_r=G\frac{dr}{dR}E_r, \qquad \tilde{E}_\phi=G\frac{r}{R}E_\phi+\frac{r}{R}\frac{dG}{dr}\frac{H}{i}. \quad (13)$$

The main difference between the standard TO and our approach is the appearance of the $G(r)$ function defined by Eq. (11). Indeed, the case of $G=1$ gives TO results: unchanged magnetic field, $\tilde{H}=H$, Eq. (12), and respective expressions for $\varepsilon_\perp$ and $\varepsilon_\parallel$, Eq. (8). By substituting $G=1$ in Eq. (11) we obtain the corresponding mapping $R=\sqrt{r^2+R_{\rm int}^2}$, the only TO mapping which transforms the virtual vacuum into a medium with μ fixed as 1. However, matching of this TO solution with vacuum at finite R, i.e., for finite thickness of hiding shell, can be reached only for trivial transformation, $R=r$.

III. NONMAGNETIC HIDING OF CYLINDRICAL OBJECTS: TRUNCATION PROCEDURE

A. Cloaking shell with infinite value of permittivity at the inner boundary

We apply this method of mapping $r \to R$ using the simplest function

$$R = R_{\text{ext}}(1 + \xi + \alpha\xi^2), \quad \xi = r/R_{\text{ext}} - 1\,, \quad \alpha < 1/2, \quad (14)$$

which satisfies the matching conditions at the outer boundary (interface with vacuum) of the cloak, $r = R_{\text{ext}}$. This mapping ensures hiding a cylindrical region with radius $R_{\text{int}} = \alpha R_{\text{ext}}$ by a nonmagnetic shell with thickness of $(1-\alpha)R_{\text{ext}}$. In Fig. 1 the radial dependence of longitudinal and transverse components of $\hat{\varepsilon}$ calculated for the parameters $\alpha = 0.3$, $k_0 R_{\text{ext}} = 20$ are shown. Inner boundary of the cloak turns out to be $k_0 R_{\text{int}} = 6$. Inset also shows the function $G(r)$, which is a solution of a differential equation (11) with $R(r)$ given by Eq. (14).

Figure 1 also illustrates the common drawback of the obtained recipe and TO formulas: A singularity of the azimuthal component of dielectric tensor appears at the boundary of the concealed region (inner boundary of the shell, R_{int}). To overcome the problem of infinite permittivity, the same procedure as in TO method can be applied. It is "truncating" the cloaking shell at certain maximal value of $\varepsilon^{\max}$. Although this makes the cloak nonideal, it still gives a substantial decrease of the scattering cross section of the object. Numerical finite-element method (FEM) simulations exhibit the efficiency of the truncated cloak as illustrated in Fig. 2. We consider a unit-electric-field TM-polarized plane wave with wave vector **k** along the x axis, $E_{\text{inc}}(X,Y) = \mathbf{y}_0 \exp(ik_0X)$, incident on a metal (perfect electric conductor, PEC, boundary conditions) cylinder of radius R_{int}. In Fig. 2(a) the distribution of the y component of electric field, $E_y(X,Y)$, is shown for the case of scattering from the PEC cylinder covered by the nonmagnetic shell designed according to Eqs. (14) and (8) and truncated at $k_0 R_{\text{int}} = 6.25$ when the transverse permittivity, $\varepsilon_\perp$, exceeds 6.78. For comparison, in Fig. 2(c) much stronger scattering of the radiation by the same metal cylinder but without the cloaking cover is shown. The effect of the cloaking cover on the scattering intensity becomes even more evident when comparing the corresponding patterns for the absolute value of scattered field, $\sqrt{|E_y - E_{\text{inc}}|^2 + |E_x|^2}$, [Figs. 2(b) and 2(d)]. Though the field scattered from the cylinder does not completely disappear, as it has to in the ideal case, the absolute value of the scattered field becomes approximately 5 times smaller (the line contours shown correspond to the scattered field absolute values of 0.2, 0.6, and 1). So one can conclude that the nonzero scattered field is caused by imperfectness of the cloak, and this imperfectness relates to two factors: (1) truncating procedure and (2) numerical discretization errors.

The obtained cloak structure is scalable: If we increase R_{ext} in formula (14) while keeping α unchanged, the calculated permittivity as a function of R/R_{ext} changes slightly. This effect is demonstrated in Fig. 3, where dependencies $\varepsilon_{rr}(R/R_{\text{ext}})$ and $\varepsilon_{\phi\phi}(R/R_{\text{ext}})$ are shown for three values of $k_0 R_{\text{ext}} = 2,\ 20,\ 20\,000$. The difference between the corresponding curves is evident only for smaller cloak ($k_0 R_{\text{ext}} = 2$), but when comparing the cases with $k_0 R_{\text{ext}} = 20$ and $k_0 R_{\text{ext}} = 20\,000$ we see actually the same shell structure. Thus, we believe that this structure can be applied for cloaking of macroscopic objects, though it cannot be confirmed by FEM simulation because of necessity for extreme numerical resources.

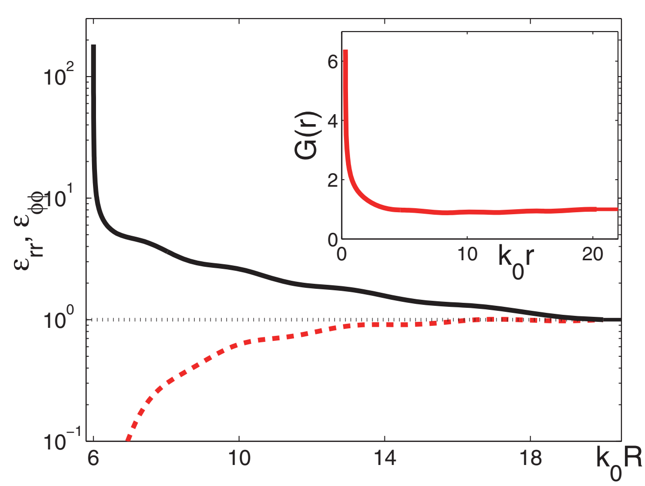

FIG. 1. (Color online) Radial structure of longitudinal, ε_{rr} (red [gray] dashed line), and transverse, $\varepsilon_{\phi\phi}$ (black solid line), components of dielectric permittivity of the medium which ensures a creation of nonmagnetic cloak for TM-polarized radiation in a cylindrical problem. The structure of the cloak is given by the mapping (14). Internal and external boundaries of the cloaking shell are $k_0 R_{\text{int}} = 6$ and $k_0 R_{\text{ext}} = 20$ respectively; at $R > R_{\text{ext}}$ the both components of $\hat{\varepsilon}$ are 1. Inset shows the corresponding dependence of scaling factor G on the "old" (virtual vacuum) radius r.

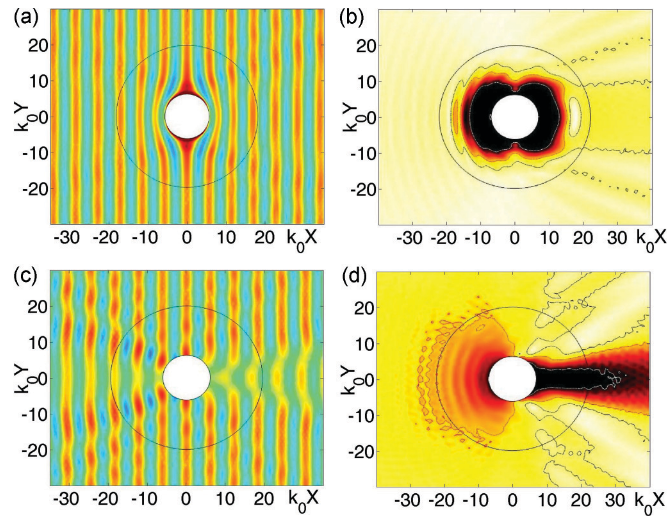

FIG. 2. (Color online) [(a), (c)] Distribution of y component of electric field, $E_y(X,Y)$, for the plane-wave scattering by a PEC cylinder of radius $R_{\text{int}} = 0.315 R_{\text{ext}}$ ($k_0 R_{\text{int}} = 6.25$); [(b), (d)] absolute value of the scattered field. Panels (a) and (b) correspond to the radiation scattering by the cylinder covered by nonmagnetic cloaking shell with the permittivity distribution ε_{rr}, $\varepsilon_{\phi\phi}$, corresponding to Fig. 1; and panels (c) and (d) correspond to the case of scattering by the bare cylinder.

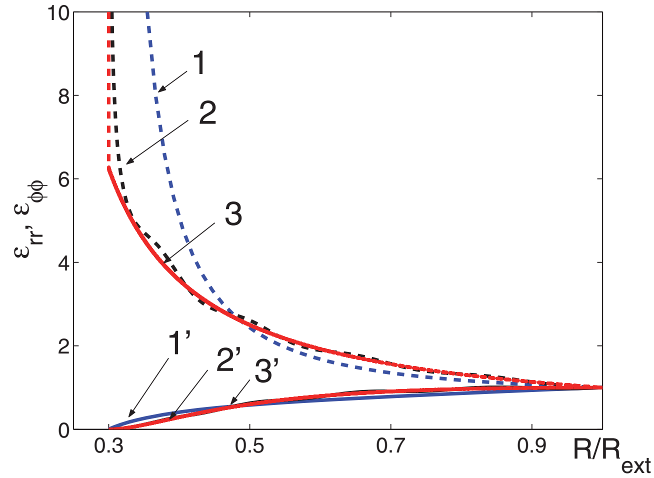

FIG. 3. (Color online) Radial structure of transverse, $\varepsilon_{\phi\phi}$ (dashed lines), and longitudinal, ε_{rr} (solid lines), components of dielectric permittivity of the medium which ensure a creation of nonmagnetic cloak for TM-polarized radiation in a cylindrical problem. The structure of the cloak is given by the mapping (14). Internal and external boundaries of the shell are $k_0 R_{\text{int}} = 0.3$ and $k_0 R_{\text{ext}} = 2$ (curves 1, 1'), $k_0 R_{\text{int}} = 3$ and $k_0 R_{\text{ext}} = 20$ (curves 2, 2'), and $k_0 R_{\text{int}} = 3\,000$ and $k_0 R_{\text{ext}} = 20\,000$ (curves 3, 3').

B. Cloaking shell with finite permittivity

The application of the truncating procedure removes the singularity in permittivity distribution, but makes the cloak imperfect, so some another way of avoiding singularity would be preferred for applications. The problem of singularity removal in material parameters of the "push-forward" cloak has been extensively discussed in the literature, and different solutions have been suggested [22–27], but all these proposals use magnetic materials.

However, for the considered type of shell it is possible to design an ideal nonmagnetic cloaking cover using only the materials with *finite permittivity*.

Formally, the origin of infinite value of $\varepsilon_\perp$ at the inner edge of the shell, $R = R_{\text{int}}$, is caused by a factor $r \to 0$ in the denominator of expression (5) for g function. The presence of a singularity at the inner edge of the shell is typical for the cloaking applications when the whole region $R < R_{\text{int}}$ is mapped onto a point $r = 0$. However, unlike TO results, the expression for $\varepsilon_\perp$ includes also a factor of $1/G^2$. So, if we set the scaling factor around the inner boundary of the shell tending to infinity, $G \to \infty$, then $\varepsilon_\perp$ can take a finite value. The detailed analysis shows that the problem of infinite permittivity can be solved if $G(r)$ in the vicinity of zero r (at the inner edge of the cloak) is chosen as

$$G(r) = A + \sqrt{a + b(\ln r/R_{\text{ext}})^2}, \quad a,b > 0. \tag{15}$$

By substituting this expression into Eq. (11) we obtain

$$\dot{R} \approx \frac{abG}{r(G - A)^3 k_0^2 R} \tag{16}$$

and therefore $\varepsilon_\perp = g/G^2 = R/(r\dot{R}G^2) \approx (k_0 R)^2 (G - A)^3/(abG^3)$. It is clear that in this case $\varepsilon_\perp$ stays constant. Furthermore, the singularity in Eq. (16) is integrable, and there is no problem with the mapping $r \to R$. In such a way, slight modification of the expression (14) around $r = 0$ allows us to obtain a distribution of permittivity tensor with the components limited by certain maximal value $\varepsilon^{\max}$: $\varepsilon_{rr}(r) < \varepsilon^{\max}$, $\varepsilon_{\phi\phi}(r) < \varepsilon^{\max}$.

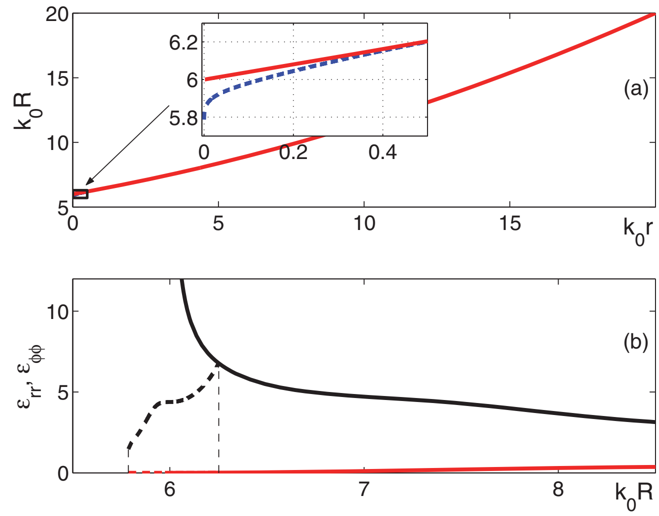

FIG. 4. (Color online) (a) Space mapping $R(r)$ (14) with the parameters of Fig. 1 (red [gray] solid line), and also the mapping modified around $r = 0$ according to formula (15) with the parameters $a = 17.98$, $b = 1.48$, $A = -5.11$ (blue [gray] dashed line); (b) corresponding unperturbed and modified distributions of the dielectric permittivity components ε_{rr}, $\varepsilon_{\phi\phi}$.

C. Structure of nonmagnetic cloak without singular values of permittivity

The dependencies $\varepsilon_\perp(R)$, $\varepsilon_\parallel(R)$ shown in Fig. 4 are the particular example of the cloaking realization with the finite material parameters $\hat{\varepsilon}$. The spatial transformation $R(r)$ has the same form as Eq. (14) for $r > r^* = 6.25/k_0$, but for $r \leqslant r^*$ it is defined by formula (15) with the parameters $a = 17.98$, $b = 1.48$, $A = -5.11$. The values of parameters in Eq. (15) are chosen to ensure the continuity of the functions G and R (and accordingly dR/dr, $\hat{\varepsilon}$) at the matching point $r = r^*$. The application of this procedure limits the permittivity in this modified layer within $6.78 > \varepsilon_{\phi\phi} > 4.71$, $\varepsilon_{rr} \approx 0$. However, it also leads to some increase of shell thickness: The boundaries of the modified region are $k_0 R = 5.79 : 6.25$, such that the size of the concealed volume reduces down to $k_0 R_{\text{int}} \approx 5.79$.

The cloaking effect obtained with this modified cover is illustrated in Fig. 5.

IV. DISCUSSION: A LIMITATION OF INVISIBILITY

It is obvious from the Fig. 5 that modification of the shell (namely, an extra layer with finite $\varepsilon_{\phi\phi}$) leads to additional reduction of scattering, but not to complete vanishing.

An analysis of far-field structure shows that in this case the scattered field is actually an azimuthally symmetric wave, and its amplitude does not converge to zero as the resolution of the computational grid is increased. The reason is simple: From Eqs. (12) and (13) it is clear that magnetic field have to vanish at $r = 0$ if $G(r = 0)$ tends to infinity according to Eq. (15), whereas the azimuthal components of electric field remains

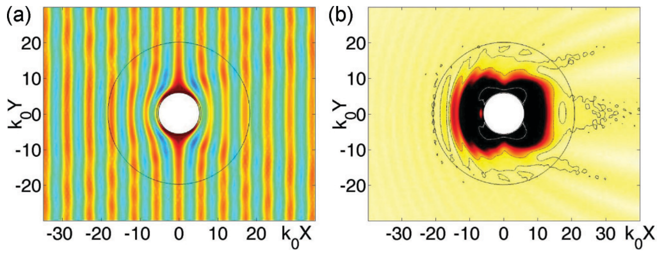

FIG. 5. (Color online) (a) Distribution of electric field $E_y(X,Y)$ for the scattering of plane wave by the metal cylinder with the radius of $R_{\rm int} = 0.29 R_{\rm ext}$ ($k_0 R_{\rm int} = 5.79$), covered by nonmagnetic cloaking shell with the tensor permittivity structure ε_{rr}, $\varepsilon_{\phi\phi}$ corresponding to Fig. 4; (b) absolute value of the scattered field.

constant, $\tilde{E}_\phi \to (r\dot{G}H)/(iR) \approx \sqrt{b}/(iR)$. This behavior evidently conflicts with PEC boundary conditions. Actually, the problem appears only for the zero-order azimuthal harmonic, such that the total scattering cross section (TSCS) may reach the maximum value of $2\lambda/\pi$. This upper limit of TSCS is rather high for the subwavelength cloaked object. However, for larger object, the ratio of the TSCS to the object size decreases and tends to zero in case of macroscopic objects.

To confirm this statement, we have calculated the TSCS as a function of geometric size of the cloaked region, $R_{\rm int} \approx \alpha R_{\rm ext}$. For a cloak design, we applied the described procedure of mapping (14) with $\alpha = 0.3$, solved Eq. (11), calculated the radial dependence of permittivity components truncated for $\varepsilon_\perp > 7$, and finally added the compensating permittivity layer corresponding to Eq. (15). The obtained permittivity profiles were used in computation of plane-wave diffraction on the cloaked PEC cylinder employing the multipolar expansion of the fields. The results are represented in Fig. 6 (solid curve), and the total scattering cross section is close to the theoretical limit of $2\lambda/\pi$ (black dotted line), the main contribution due to scattering of the zero-order mode (≈86%). For comparison, the scattering characteristics of the truncated cloaking shell are shown also in Fig. 6 (dashed curve), and the main contribution is due to scattering of the first-order (dipole) mode (≈96%). It turns out that the truncated cloak operates better than ideal [28]; this paradoxial point is due to the fact that the size of truncated region in virtual r space, r_{tr}, is small, such that multipoles with the azimuthal number more than 1 do not scatter, and the dipole scattering cross section is less than $2\lambda/\pi$. This is an interesting and specific point because in the standard TO approach increase of $R_{\rm int}$ induces the proportional increase of the truncated region, $r_{tr} \sim R_{\rm int}/\varepsilon_\perp^{\rm max}$, and respective growth of the visibility if the maximum value of $\varepsilon_\perp$, $\varepsilon_\perp^{\rm max}$, is fixed. On the contrary, it is clear from Fig. 6 that the proposed nonmagnetic design ensures nearly constant value of r_{tr} when $R_{\rm int}$ increases. Moreover, this effect can be confirmed analytically. Indeed, with the used mapping (14) we have finite value of $\dot{R} = 1 - 2\alpha$ at $R = R_{\rm int}$, and Eq. (11) allows one to find the behavior of the G function in the vicinity of $r = 0$ ($R \approx R_{\rm int}$): It tends to zero as $G \approx A\sqrt{r}$ with the amplitude $A = 2k_0\sqrt{R_{\rm int}\dot{R}}$. By substituting these expressions in Eq. (8) we obtain an estimation for r_{tr},

$$r_{tr} \approx (2k_0\dot{R}\sqrt{\varepsilon_\perp^{\rm max}})^{-1},$$

and it truly does not depend on $R_{\rm int}$. This result motivates more detailed investigation of the effect and its real application for macroscopic cloaking.

By comparing the expressions for transverse permittivity in the vicinity of $r = 0$ obtained in TO theory, $\varepsilon_\perp^{TO} = R/(r\dot{R})$, and for square root of transverse permittivity in

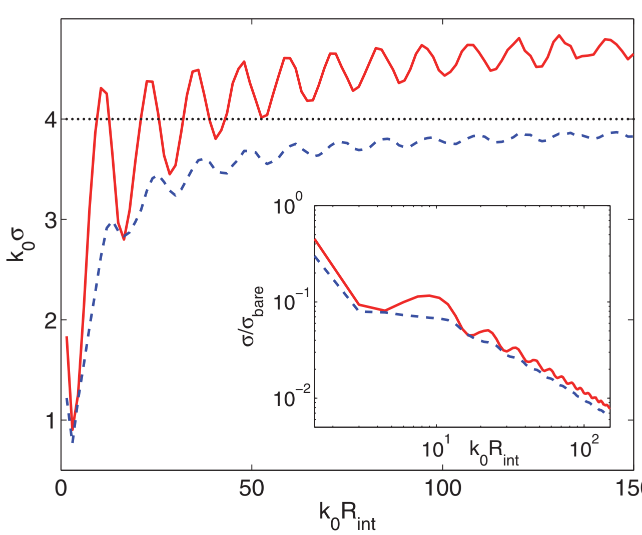

FIG. 6. (Color online) Total scattering cross section $k_0\sigma$ as a function of cloaked size, $k_0 R_{\rm int}$; red (gray) solid curve corresponds to the ideal cloaking shell (with added compensating layer); blue (gray) dashed curve corresponds to the truncated at $\varepsilon_\perp = 7$ permittivity profile; and black dotted line is the theoretical limit $2k_0\lambda/\pi = 4$. Inset shows the respective ratios of the TSCS to the scattering cross section of the bare PEC cylinder.

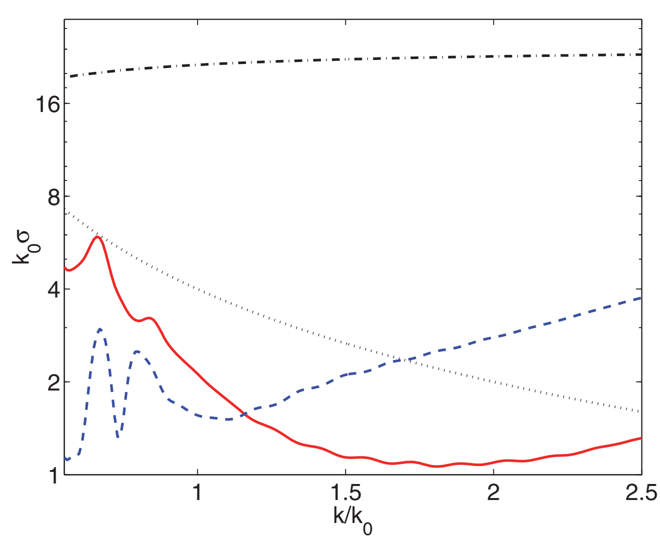

FIG. 7. (Color online) Total scattering cross-section $k_0\sigma$ as a function of the normalized wave number, k/k_0; red (gray) solid curve corresponds to the ideal cloaking shell (with added compensating layer); blue (gray) dashed curve corresponds to the truncated at $\varepsilon_\perp = 7$ permittivity profile; black dash-dotted line corresponds to the scattering from bare metallic cylinder; and black dotted line is the theoretical limit $2k_0\lambda/\pi = 4$.

our nonmagnetic design, when $G \approx 2k_0\sqrt{R_{\rm int}}\dot{R}\sqrt{r}$, $\sqrt{\varepsilon_{\perp}^{NM}} \approx \sqrt{R}/(2k_0 r\dot{R}\sqrt{R_{\rm int}}) \approx \lambda/(4\pi r\dot{R})$, we see very similar formulas, though in our case the role of the size of cloaked region, $R \approx R_{\rm int}$, plays a value given by $\lambda/(4\pi)$. Thus, unlike TO, our design is evidently tuned to the specific wavelength. Dispersion behavior of scattering characteristics was studied numerically; however, the dispersion of near-zero medium was not taken into account, and we supposed $\hat{\varepsilon}$ to be frequency independent. Figure 7 shows the dependence of TSCS on the normalized wave number.

We see that the spectral dependence of TSCS is not resonant and the cloak is rather broadband in this approximation.

V. CONCLUSION

In conclusion, it has been shown that nearly ideal nonmagnetic invisibility cloaking of cylindrical objects with respect to TM-polarized electromagnetic wave is quite feasible. The cloaking shell does not contain any materials with extremely high dielectric permittivity and it is scalable, which potentially makes possible experimental observation of the cloaking effect for macroscopic sizes of hidden objects. The developed approach can be easily implemented for design of nonmagnetic devices analogous to multiple TO ones. This work takes one more step toward highly effective devices based upon existing materials for electromagnetic wave manipulations at micro as well as macro scales.

ACKNOWLEDGMENTS

The authors thank Yu. S. Kivshar for useful discussions. This work was supported in part by RFBR through Grants No. 13-02-97115 and No. 13-02-00881.

[1] J. B. Pendry, D. Schurig, and D. R. Smith, Science **312**, 1780 (2006).
[2] U. Leonhardt, Science **312**, 1777 (2006).
[3] D. Schurig, J. J. Mock, B. J. Justice, S. A. Cummer, J. B. Pendry, A. F. Starr, and D. R. Smith, Science **314**, 977 (2006).
[4] A. Alu and N. Engheta, Phys. Rev. E **72**, 016623 (2005).
[5] A. Alu and N. Engheta, J. Appl. Phys. **97**, 094310 (2005).
[6] A. Alu and N. Engheta, Phys. Rev. Lett. **100**, 113901 (2008).
[7] A. A. Zharov and N. A. Zharova, Bull. Russ. Acad. Sci.: Phys. **74**, 89 (2010).
[8] D. S. Filonov, A. P. Slobozhanyuk, P. A. Belov, and Yu. S. Kivshar, Phys. Status Solidi RRL **6**, 46 (2012).
[9] A. Koray, I. Bulu, K. Guven, M. Kafesaki, C. M. Soukoulis, and E. Ozbay, New J. Phys. **7**, 168 (2005).
[10] D. P. Gaillot, C. Croenne, and D. Lippens, Opt. Express **16**, 3986 (2008).
[11] J. Andkjar, N. A. Mortensen, and O. Sigmund, Appl. Phys. Lett. **100**, 101106 (2012).
[12] C. A. Valagiannopoulos and P. Alitalo, Phys. Rev. B **85**, 115402 (2012).
[13] W. Yan, M. Yan, and M. Qiu, Appl. Phys. Lett. **93**, 021909 (2008).
[14] L. H. Gabrielli, J. Cardenas, C. B. Poitras, and M. Lipson, Nat. Photon. **3**, 461 (2009).
[15] H. Chen, B. Zheng, L. Shen, H. Wang, X. Zhang, N. Zheludev, and B. Zhang, arXiv:1306.1780.
[16] J. Li and J. B. Pendry, Phys. Rev. Lett. **101**, 203901 (2008).
[17] D. Bao, K. Z. Rajab, Y. Hao, E. Kallos, W. Tang, C. Argyropoulos, Y. Piao, and S. Yang, New J. Phys. **13**, 103023 (2011).
[18] J. Valentine, J. Li, T. Zentgraf, G. Bartal, and X. Zhang, Nat. Mater. **8**, 560 (2009).
[19] J. Renger, M. Kadic, G. Dupont *et al.*, Opt. Express **18**, 15758 (2010).
[20] W. Cai, U. K. Chettiar, A. V. Kildishev, and V. M. Shalaev, Nat. Photon. **1**, 224 (2007).
[21] W. Cai, U. K. Chettiar, A. V. Kildishev, V. M. Shalaev, and G. W. Milton, Appl. Phys. Lett. **91**, 111105 (2007).
[22] Z. Ruan, M. Yan, C. W. Neff, and M. Qiu, Phys. Rev. Lett. **99**, 113903 (2007).
[23] M. Yan, Z. Ruan, and M. Qiu, Phys. Rev. Lett. **99**, 233901 (2007).
[24] T. Tyc and U. Leonhardt, New J. Phys. **10**, 115038 (2008).
[25] U. Leonhardt, and T. Tyc, Science **323**, 110 (2009).
[26] J. Hu, X. M. Zhou, and G. K. Hu, Appl. Phys. Lett. **95**, 011107 (2009).
[27] W. X. Jiang, T. J. Cui, X. M. Yang, R. Liu, and D. R. Smith, Appl. Phys. Lett. **93**, 194102 (2008).
[28] Seemingly stronger plane-wave scattering by the truncated cloaking shell compared to the "ideal" one in Fig. 5 is related to its dipole character. As a result the maximum of the scattered radiation falls on the forward and back scattering, and this maximum exceeds locally the azimuthally uniform (monopole) scattering by the "ideal" shell. However, in terms of total cross section the truncated cloak operates better.